

UNCLASSIFIED

Defense Technical Information Center
Compilation Part Notice

ADP010493

TITLE: Integral Control of Large Flexible
Aircraft

DISTRIBUTION: Approved for public release, distribution unlimited

This paper is part of the following report:

TITLE: Structural Aspects of Flexible Aircraft
Control [les Aspects structuraux du controle
actif et flexible des aeronefs]

To order the complete compilation report, use: ADA388195

The component part is provided here to allow users access to individually authored sections of proceedings, annals, symposia, ect. However, the component should be considered within the context of the overall compilation report and not as a stand-alone technical report.

The following component part numbers comprise the compilation report:

ADP010474 thru ADP010498

UNCLASSIFIED

Integral Control of Large Flexible Aircraft

Klaus König

Jörg Schuler

DaimlerChrysler Aerospace Airbus GmbH

Hünefeldstraße 1-5

28183 Bremen

Germany

SUMMARY

In a flexible aircraft flight control, load control and structural mode control interfere with each other. Therefore, an integral design of controller(s) is necessary. This paper describes how an integral aircraft model covering the requirements of all three disciplines can be derived and how an integral controller can be designed by multiobjective parameter optimization. General design criteria for mode control are proposed.

1. INTRODUCTION

Flight control and aeroelastics are two disciplines for aircraft (a/c) design which have worked more or less independently from each other in the past. Flight control deals with the nonlinear rigid-body motion of the a/c and aeroelastics deals with linear vibrations of the a/c structure.

This was possible as long as the eigenfrequencies of rigid-body motion and structural vibrations were clearly separated from each other and slow movements of control surfaces were sufficient. But with modern large and flexible a/c there are interferences of both types of motion.

There are three reasons for this.

First the eigenfrequencies of rigid-body motion and structural vibrations come close together causing stronger cross coupling. Second the measured input signals of the electronic flight control system (EFCS) might contain signal parts of structural vibrations. Feeding back these signals could therefore lead to instability of flutter.

Third there may be the phenomenon of aircraft pilot coupling (APC) where vibrations of the cockpit floor structure may lead to movements of the side stick via pilot seat and pilot body/pilot arm, thereby causing control surface movements with eigenfrequencies of the rigid-body and the a/c structure.

With modern a/c it is therefore no longer possible to neglect the coupling between rigid-body motions and deflections of the structure. Interdisciplinary cooperation of flight control, aeroelastics and of the discipline loads prediction is therefore required. An integral a/c model and an integral controller covering the requirements of all these disciplines are necessary for a successful a/c design.

In the following some details of integral model derivation and some remarks on the design of integral controllers are given. Emphasis is put on the structural vibrations part of this controller.

2. THE INTEGRAL MODEL

The integral mathematical model of the a/c must include rigid-body movements and structural vibrations. This causes problems. In the past rigid-body movements studied by flight mechanics covered large movements such as large angles of attack, and this required nonlinear aerodynamics and nonlinear Euler-Newton equations. Elasticity or structure deformation was only introduced via "elastified" aerodynamic coefficients taking into consideration steady state deflections of the a/c structure.

On the contrary, structural vibrations studied by aeroelastics were described by linear equations paying attention to the first harmonics of unsteady aerodynamics with small amplitudes of angle of attack and neglecting completely aerodynamic forces in fore and aft direction. Therefore, rigid-body motion is included – if at all – in these linear equations only in a rather rough manner.

An integral model covering the requirements of both disciplines may therefore be rather complicated. It should superimpose small deflections of the grid point masses of a huge FE-model with large three-dimensional movements in space. It should take into account aerodynamic loads due to large angles of attack and large amplitudes of the phugoid for 100000 degrees of freedom. In addition, Navier-Stokes CFD codes and nonlinear Euler-Newton inertias should be implemented. But for the time being,

another approach is necessary.

One of the most obvious models is therefore a linear model valid for a working point under steady state flight conditions. This allows the study of movements around this point, and flights within the whole envelope are possible by interpolation between different working points.

The model presented here is based on the traditional aeroelastics model in frequency domain. But it has been improved so that its rigid-body modes should approach the modes of the linearized flight mechanics model. The improved model includes the following:

- 1 stiffness matrix of structure
- 2 inertia matrix including all grid points
- 3 aerodynamic panels, also for the fuselage
- 4 steady state air loads at the working point
- 5 steady state elastic deformations of the structure
- 6 corrections of the stiffness matrix due to steady state deformations
- 7 corrections of the inertia matrix due to steady state deformations
- 8 eigenvalue analysis of the structure (without aerodynamics)
- 9 mode reduction by truncation
- 10 addition of control modes for compensation of truncation effects
- 11 transformation of rigid-body modes from main inertia axes to geodetic aircraft reference axes
- 12 traditional unsteady air loads
- 13 addition of missing elements to traditional unsteady air loads
- 14 inclusion of gust loads
- 15 smoothing of rigid-body air loads at zero frequency
- 16 engine loads
- 17 weight force
- 18 structural damping
- 19 linearization and transformation into time domain
- 20 eigenvalue analysis at working point
- 21 introduction of nonlinear rigid-body motion
- 22 installation of actuators
- 23 if wanted, transformation of rigid-body modes into completely moving coordinates of flight mechanics
- 24 if wanted, further mode reduction for use in flight simulators
- 25 addition of aircraft pilot coupling (APC) transfer functions
- 26 addition of electronic flight control system (EFCS)

Items - 1, 2, 3 (partially), 8, 9, 12, 18, 20 are already covered by classical aeroelastic analyses. Items -10, 22, 26 are to be added at least for the analysis of "structural coupling of EFCS". The others are recommended for integral control design and analysis.

In the following some of these items are discussed in more detail.

2.1 Aerodynamic Panels (-3)

Classical aeroelastics most often neglects the air loads of the fuselage. This is not sufficient for an integral model. The inclusion of a panel cross (s. Fig. 2.1-1) with vertical and horizontal panels may be the most simple approach if loads caused by roll movements are excluded and if all loads are scaled (from panel to cylinder loads). A scaling factor of 0.5 was sometimes found by experience.

2.2 Stiffness and Inertia Corrections (-6, -7)

They are second order effects, but their realization is rather simple. It simply requires the multiplication of the original stiffness and inertia matrices from the right and the left side by a transposition matrix resulting from steady state structure deformations.

2.3 Control Modes (-10)

A classical flutter analysis includes about 100 modes with the lower frequencies of a system of about 100000 degrees of freedom. Due to this truncation, local stiffnesses may be lost. But just such local connection stiffnesses may be important if control surfaces are to be moved via EFCS by actuator loads. Therefore, assumed modes according to Rayleigh-Ritz are added. These modes are defined by a unit deflection of the actuator and the resulting deflections of the other grid points of the structure. These modes are called control modes and are to be introduced in addition to the classical rotation modes of the control surfaces. With rigid aircraft both modes would be identical. More details about the influence of control modes are given in ref. 1.

2.4 Unsteady Air Loads (-13)

Until now traditional unsteady air loads are e.g. NASTRAN doublet lattice air loads. These are the first harmonics for a panel oscillating in an air stream. The initial angle of attack is zero and the Mach number (Ma) is constant. Therefore, the following loads are not covered:

- in plane loads (mainly fore and aft drag and side loads)
- unsteady loads due to
 - in plane movements (mainly fore and aft)
 - air density ρ varying with altitude
 - Mach number varying with altitude and velocity.

For an integral model this approximation is not sufficient. If better air loads (e.g. from CFD codes) are not available, some corrections are necessary. Details for this are given in ref. 2. Here it can be stated that steady state air loads p_0 —also computed by the doublet lattice method in NASTRAN for each aerodynamic panel—can be used to establish the missing elements. This results in the following:

For lift forces resulting from steady state drag loads

$$\Delta p_z = -p_0 x \cdot \Delta z / \bar{x}_0 \quad 2.4-1$$

For negative drag loads (induced drag, neglecting friction)

$$\Delta p_x \approx (\Delta p_z) \cdot \alpha_0 - p_0 z \cdot \Delta z / \bar{x}_0 \quad 2.4-2$$

For side loads

$$\Delta p_y \approx -p_0 z \cdot \Delta \varphi + p_0 x \cdot \Delta \dot{y} / \bar{x}_0 \quad 2.4-3$$

For in plane movements

$$\Delta p(\dot{x}) \approx \frac{p_0}{\bar{x}_0^2} \cdot 2 \cdot \dot{x}_0 \cdot \Delta \dot{x} \quad 2.4-4$$

For dependencies from Q and Ma

$$\Delta p(Q) \approx \frac{p_0(Q_2(z_2)) - p_0(Q_1(z_1))}{z_2 - z_1} \cdot \Delta z \quad 2.4-5$$

$$\Delta p(Ma) \approx \frac{p_0(Ma_2) - p_0(Ma_1)}{Ma_2 - Ma_1} \cdot \left(\frac{\Delta \dot{x}}{a_0} - \frac{Ma_0}{a_0} \cdot \frac{a(z_2) - a(z_1)}{z_2 - z_1} \cdot \Delta z \right) \quad 2.4-6$$

Another deficit to be mentioned here are the doublet lattice air loads of control surfaces. Usually, they are too large and should be corrected to wind tunnel results of hinge moments. But the corrections must also include the airfoil in front of the control surface. Correction factors of up to 0.6 are possible.

2.5 Smoothing of Rigid-Body Air Loads at Zero Frequency (-15)

If steady state air loads from wind tunnel measurements are available, it should be possible to improve the doublet lattice air loads of rigid-body modes at zero frequency. This can be done by separating these loads by an eigenvalue analysis. After transformation of the separated doublet lattice air loads into the coordinate system of the measurement, these loads can be substituted by Fourier-transformed air loads measured for zero frequency and the smallest non-zero frequency.

For the other frequencies a smoothed change to doublet lattice air loads can be chosen. For a linear smoothing this yields:

$$p = p_{\text{measured}}(\omega) \text{ if } \omega < \omega_1$$

$$p = p_{\text{measured}}(\omega) \cdot \frac{(\omega_r - \omega)}{(\omega_r - \omega_1)} + p_{\text{doublet lattice}}(\omega) \cdot \frac{(\omega - \omega_1)}{(\omega_r - \omega_1)} \text{ if } \omega_1 \leq \omega \leq \omega_r$$

$$p = p_{\text{doublet lattice}}(\omega) \text{ if } \omega > \omega_r$$

2.6 Engine Loads and Weight Forces (-16, -17)

Loads such as gross thrust, ram drag and gravity weight are not included in aeroelastic analyses, but they are of influence for flight mechanics. Therefore, they must be introduced.

As to the engines, their unsteady load portion is due to three different reasons:

First from the unsteady movement of the engine position and its steady state loads, i.e. due to the change of direction (T'_{ePo}) and due to transposition (V'_{Ea0})

$$p_0 + \Delta p = V'_{Eo0} \cdot T'_{eEo} \cdot p_{0eE}$$

resulting in

$$\Delta p = -FP(p_{0eE}) \cdot \Delta r_{oE} \quad 2.6-1$$

with

$$FP(p_{0eE}) = \begin{bmatrix} 0 & 0 & 0 & 0 & -p_0 z & p_0 y \\ 0 & 0 & 0 & p_0 z & 0 & -p_0 x \\ 0 & 0 & 0 & -p_0 y & p_0 x & 0 \\ 0 & -p_0 z & p_0 y & 0 & 0 & 0 \\ p_0 z & 0 & -p_0 x & 0 & 0 & 0 \\ -p_0 y & p_0 x & 0 & 0 & 0 & 0 \end{bmatrix}; \Delta r_{oE} = \begin{bmatrix} \Delta x \\ \Delta y \\ \Delta z \\ \Delta \varphi \\ \Delta \theta \\ \Delta \psi \end{bmatrix}$$

Second from their derivatives due to velocity and altitude changes as the air loads (2.4-5, -6)

$$\Delta p = \frac{p_0(Ma_2) - p_0(Ma_1)}{Ma_2 - Ma_1} \cdot \left(\frac{\Delta \dot{x}}{a_0} - \frac{Ma_0}{a_0} \cdot \frac{a(z_2) - a(z_1)}{z_2 - z_1} \cdot \Delta z \right) + \frac{p_0(Q_2(z_2)) - p_0(Q_1(z_1))}{z_2 - z_1} \cdot \Delta z \quad 2.6-2$$

Third from their derivatives due to control inputs

$$\Delta p = \frac{p_0(n_2) - p_0(n_1)}{n_2 - n_1} \cdot \Delta n \quad 2.6-3$$

The weight must be introduced if the final equations are transformed from the geodetic (g) to the moving coordinate system (f)

$$\Delta g_f = g_g \cdot \begin{bmatrix} -\Delta \theta \cdot \cos \varphi_0 \cdot \cos \theta_0 + \Delta \psi \cdot \sin \varphi_0 \cdot \cos \theta_0 \\ \Delta \psi \cdot \cos \varphi_0 \cdot \cos \theta_0 - \Delta \psi \cdot \sin \theta_0 \\ -\Delta \varphi \cdot \sin \varphi_0 \cdot \cos \theta_0 + \Delta \theta \cdot \sin \theta_0 \end{bmatrix} \quad 2.6-4$$

2.7 Linearization and Transformation into Time Domain (-19)

For the purpose of controller design, the subsequent inclusion of nonlinearities or the use in flight simulators, the integral model is required in time domain. When starting with the aeroelastic model in frequency domain, a linearization of air loads and a transformation are necessary. Methods for this were proposed by Vepa (s. ref. 3), Roger (s. ref. 4) or Karpel (s. ref. 5). Especially the minimum state method of Karpel was successfully used, though it requires a larger amount of computing. Fig. 2.7-1 shows an example of good approximation.

2.8 Introduction of Nonlinear Rigid-Body Motion (-21)

All the improvements mentioned above may not be sufficient for a precise rigid-body movement as required by flight mechanics. Therefore, a substitution of the improved "aeroelastic" rigid-body motion by the "flight mechanics" motion is recommended. In this process a nonlinear rigid-body movement can also be introduced.

Of course this substitution must only be done for the decoupled orthogonal modes followed by a modal retransformation to the original coordinates.

By starting from the aeroelastics equation

$$\dot{x}A = AA \cdot xA + BA \cdot u \quad 2.8-1$$

with

$$xA = \begin{bmatrix} xAr \\ xAe \end{bmatrix} = \phi A \cdot \begin{bmatrix} qAr \\ qAe \end{bmatrix}$$

$$\psi A = \phi A^{-1}$$

resulting in the orthogonal coordinates

$$\begin{bmatrix} \dot{q}Ar \\ \dot{q}Ae \end{bmatrix} = \begin{bmatrix} \lambda Ar & 0 \\ 0 & \lambda Ae \end{bmatrix} \cdot \begin{bmatrix} qAr \\ qAe \end{bmatrix} + \begin{bmatrix} \psi A_{rr} \cdot BAr + \psi Ae \cdot BAe \\ \psi Ae \cdot BAr + \psi Ae \cdot BAe \end{bmatrix} \cdot u \quad 2.8-2$$

with the eigenvalues

λAr (rigid) and λAe (elastic)

and defining

$$xFr = \phi A_{rr} \cdot qAr \quad 2.8-3$$

as intended by traditional flight mechanics,

one obtains with equation 2.8-2

$$\dot{x}Fr = \phi A_{rr} \cdot \lambda Ar \cdot \phi A_{rr}^{-1} \cdot xFr + \phi A_{rr} \cdot (\psi A_{rr} \cdot BAr + \psi Ae \cdot BAe) \cdot u \quad 2.8-4$$

Further on it results after some rearrangements:

$$\begin{bmatrix} \dot{x}Ar \\ \dot{x}Ae \end{bmatrix} = \begin{bmatrix} 1 \\ \phi Ae \cdot \phi A_{rr}^{-1} \end{bmatrix} \cdot \dot{x}Fr + \begin{bmatrix} \phi Ae \cdot \lambda Ae \cdot \psi Ae & \phi Ae \cdot \lambda Ae \cdot \psi Ae \\ \phi Ae \cdot \lambda Ae \cdot \psi Ae & \phi Ae \cdot \lambda Ae \cdot \psi Ae \end{bmatrix} \cdot \begin{bmatrix} xAr \\ xAe \end{bmatrix} + \begin{bmatrix} \phi Ae \cdot (\psi Ae \cdot BAr + \psi Ae \cdot BAe) \\ \phi Ae \cdot (\psi Ae \cdot BAr + \psi Ae \cdot BAe) \end{bmatrix} \cdot u \quad 2.8-5$$

Briefly, equation 2.8-4 and -5 can be written as follows:

$$\begin{bmatrix} \dot{x}Fr \\ \dot{x}Ar \\ \dot{x}Ae \end{bmatrix} = \begin{bmatrix} A_{rr} & 0 & 0 \\ A_{rr} & A_{rr} & A_{rr} \\ \phi Le \cdot A_{rr} & A_{rr} & A_{rr} \end{bmatrix} \cdot \begin{bmatrix} xFr \\ xAr \\ xAe \end{bmatrix} + \begin{bmatrix} B_{rr} \\ B_{rr} + B_{rr} \\ \phi Le \cdot B_{rr} + B_{rr} \end{bmatrix} \cdot u$$

or

$$\dot{x}I = AI \cdot xI + BI \cdot u \quad 2.8-6$$

That is the integral equation of aeroelastics and flight mechanics. If required, A_{rr} and B_{rr} (implying ϕ_{rr} and λ_{rr}) may be taken from flight mechanics or the nonlinear $\dot{x}Fr = f(xFr, u)$ of flight mechanics may be introduced. In any case, it is the most reasonable compromise. It keeps the eigenvalues of the rigid a/c λ_r of the discipline defining xFr and keeps the eigenvalues of the elastic structure λ_e of aeroelastics unchanged as can easily be proven. Even simulations in a moving simulator with elasticity included can be performed. The eigenvector matrix of AI reads:

$$\begin{bmatrix} (\phi_{rr} \text{ or } \phi_{rr}) & 0 & 0 \\ (\phi_{rr} \text{ or } \phi_{rr}) & -1 & \phi Ae \\ \phi Ae \cdot \phi Ae^{-1} \cdot (\phi_{rr} \text{ or } \phi_{rr}) & -\phi Ae \cdot \phi_{rr} & \phi Ae \end{bmatrix}$$

and their eigenvalue matrix:

$$\begin{bmatrix} (\lambda Fr \text{ or } \lambda Ar) & \\ 0 & \lambda Ae \end{bmatrix} \quad 2.8-7$$

2.9 Installation of Actuators (-22)

Actuators are highly nonlinear elements, mainly due to the viscous damping effect of the oil flow, the overlapping of the throttle

orifices and the quantization effects of the digital servo control loop. Therefore, actuators have to be substituted by their frequency response functions (in the following called transfer functions), if linear systems are to be used. This includes the first harmonic but neglects all higher orders or subharmonic responses. Then a decision has to be taken on the actuator model. There are two possibilities for actuators with closed control loop.

The stroke model:

$$zA = H_{zA,u} \cdot u \quad 2.9-1$$

and the load model:

$$zA = H_{zA,u} \cdot u + H_{zA,pA} \cdot pA \quad 2.9-2$$

where zA = realized actuator stroke

u = commanded actuator stroke

pA = actuator action load

$H_{..}$ = transfer function

($H_{zA,u}$ may be called "frequency response function of control" and $H_{zA,pA}$ "frequency response function of disturbance")

and after some rearrangements of equation 2.9-2 for the loads model:

$$pA = pH - k_A \cdot zA \quad 2.9-3$$

with

$$pH = H_{pH,u} \cdot u + H_{pH,zA} \cdot zA$$

$$H_{pH,u} = -H_{zA,pA}^{-1} \cdot H_{zA,u}$$

$$H_{pH,zA} = H_{zA,pA}^{-1} + k_A$$

k_A = chosen more or less arbitrarily

Both models have their advantages and disadvantages.

2.9-1 The stroke model

This is the simpler model and the one most often used. It requires the elimination of zA , the actuator stroke or deflection, from aircraft structure equations and its transfer to the right side of these equations to make it available as excitation.

The remaining homogenous equations of structure on the left side do no longer include actuators. They are only valid for rigid actuators or rigid connections between control surface and aircraft.

Therefore, two eigenvalue calculations are required. The usual one for classical flutter analyses without electronic control but with flexible actuators and the other one for flutter analyses with electronic control and with rigid actuators. Most probably, the eigenfrequencies and mode shapes of these two models will vary to a greater extent.

The models represent two different working points. The one with rigid actuator may be too far away from the conditions needed later when the actuator is flexible and moved by electronic control.

Besides, it should also be mentioned that in case of polynomial approximations of the transfer function of the stroke model, the order of the denominator polynomial must be two orders higher than the nominator polynomial to get accelerations of actuator stroke from commanded stroke.

2.9-2 The loads model

This model is the more complicated one. Its advantage is that it allows the inclusion of actuator flexibility existing under dynamic conditions. The model operates as a real linear spring and a disturbance load pH in parallel. If the spring term $-k_A \cdot zA$ of equation 2.9-3 is brought to the left side of aircraft structure equations, a classical eigenvalue calculation with flexible actuators can be performed and one set of modes can be used for flutter analyses with and without electronic control. This is a second advantage of the loads model. The stiffness k_A (and perhaps even an additional damping term) can be taken from ground vibration tests. A third advantage could be the fact that the introduction of $H_{pH,zA}$ in principle allows a stiffness correction even after modal truncation, as explained already in ref. 1.

The control term $H_{pH,u} \cdot u$ and the difference between complex and real negative active spring $(H_{zA,pA}^{-1} + k_A) \cdot zA$ remain on the right side of aircraft equations. An example of the negative complex spring "stiffness" $H_{pA,zA}$ is given in Fig. 2.9-1, together with a chosen real substitute $-k_A$. The differences are not negligible.

Fig. 2.9-2 gives some information about the influence of different terms of the actuator transfer function. It shows a vertical wing tip

acceleration response due to elevator movement in flight. Three cases are shown. The first one for the complete actuator model with

$$\begin{aligned} H_{pH,u} &= -H_{zA,pA}^{-1} \cdot H_{zA,u} \\ H_{pH,zA} &= H_{zA,pA}^{-1} + k_A \end{aligned}$$

the second one arbitrarily with

$$\begin{aligned} H_{pH,u} &= -H_{zA,pA}^{-1} \cdot H_{zA,u} \\ H_{pH,zA} &= 0 \end{aligned}$$

the third simplified one with

$$\begin{aligned} H_{pH,u} &= k_A \cdot H_{zA,u} \\ H_{pH,zA} &= 0 \end{aligned}$$

In the figure the peaks of structural response are clearly visible. The second case shows large deviations at about 17 Hz, while for the third case, only small deviations at about 8 Hz are visible. So it can be concluded that the complex frequency response function of disturbance $H_{zA,pA}$ has a larger influence and should be precise enough, if used.

2.9-3 Scatter

Another important factor of actuator models is the large number of influence parameters, such as

- ☐ temperature, environment
- ☐ backlash, wearing
- ☐ supply and return pressure
- ☐ servo control law (gain, sample rate)
- ☐ activated mode
- ☐ amount of mass to be moved
- ☐ static load in working point
- ☐ static position in working point
- ☐ amplitude and frequency of command
- ☐ amplitude and frequency of external load
- ☐ failure conditions
 - supply pressure decrease
 - leakage
 - wrong activation status
 - desynchronization of multiple actuators
 - mechanical blocking or fracture
 - air in hydraulic oil

Therefore, a broad scatter band of transfer functions is to be expected. The influence of this scatter is shown in Fig. 2.9-3. The same transfer function as the one shown in Fig. 2.9-2 is given for the complete actuator model, together with its upper and lower tolerance (mainly due to oil temperatures of 90°, 35° and -15°). The differences are dramatic. As a consequence, stability and response analyses must include a reasonable amount of scatter.

2.10 Transformation into Completely Moving Coordinates (-23)

Flight mechanics use a coordinate system which moves completely with deflection. Aeroelastics use an inertial geodetic coordinate system. The integral model derived from aeroelastics starts with the inertial system. Therefore, a transformation may sometimes be necessary. For the sake of completeness, it should be mentioned here that any transformation into the flight mechanics system adds so-called Euler terms to the equations. They can simply be derived as follows:

If

$$\dot{s}_{ft} = T_{fAg} \cdot \dot{s}_{gt} \quad 2.10-1$$

with

\dot{s}_{gt} velocity with components measured in the inertial coordinate system g
 \dot{s}_{ft} same velocity, but its components are now measured in the completely moving coordinate system f .

T_{fAg} matrix of coordinate transformation from g to f with Euler angles

the following results:

$$\ddot{s}_{ft} = \ddot{T}_{fAg} \cdot \dot{s}_{gt} + T_{fAg} \cdot \ddot{s}_{gt} \quad 2.10-2$$

with the first term being the Euler term (derived without cross products or special derivation symbols for derivation in moving coordinate systems!). The Euler term is not negligible since \dot{s}_{gt} in-

cludes the velocities of the aircraft. All the other terms contain small variables.

2.11 Addition of Aircraft Pilot Coupling (APC), (-25)

In classical aeroelastics the movement of an aircraft is determined exclusively by the aircraft structure and the air. But with highly flexible a/c, a pilot in the loop must also be investigated.

If e.g. the floor of the aircraft cabin is vibrating, this vibration is transferred via seat, pilot body and arm to the side stick. The side stick is unintentionally moved and introduces signals to the actuators deflecting the control surfaces which excite the aircraft via air loads and closes the loop of vibration (s. Fig. 2.11-1).

This is not only of theoretical interest, critical cases – called PIO cases before – are known from several aircraft.

Therefore, the complete integral model should include this bio-mechanical closed loop circuit of APC.

This can be done if a transfer function from aircraft cabin floor vibration to stick input is available. Such functions were recently measured and some are published in ref. 6. Fig. 2.11-2 shows an example.

If everything mentioned up to now is introduced, the integral model is ready for design and application of integral control.

2.12 Results from an Integral Model

An aircraft model including most of the effects mentioned above was established and its characteristics were studied.

Based on flight mechanics, three different sets of linearized rigid-body models were available. An early one F1Lr, an improved one with "rigid" aerodynamic coefficients F2Lr and one with "elasticified" aerodynamic coefficients F2Le.

Based on aeroelastics, three different sets of models are available. The first one A(qr) includes only rigid-body modes, the second one A(qs) includes the first six symmetric and six antisymmetric elastic modes, and the third one A(qc) includes two times 27 instead of 12 elastic modes.

2.12-1 Eigenvalues

Table 2.12-1 gives a survey of the eigenvalues (frequency f_n and damping ξ_n) of the most important rigid-body modes.

For the "short period" the frequencies of flight mechanics are in general smaller than the frequencies of aeroelastics, while the dampings show opposite tendencies. Elastic a/c show smaller frequencies and larger dampings for both disciplines. The influence of elasticity is not negligible.

For the "dutch roll" the frequencies are in better agreement, where as the dampings of flight mechanics show larger scatter. The influence of elasticity is smaller.

The "phugoid" is rather sensitive and a larger scatter is visible for the values of flight mechanics. Nevertheless, the frequencies of aeroelastics do not differ so much. The influence of elasticity is visible.

The other aperiodic rigid-body modes show relatively good approximation. The increase of the number of elastic modes to 54 has minor influences on the frequencies and dampings of the first 12 elastic modes.

2.12-2 Response to Control Inputs

Figures 2.12-1 to -4 show examples of time response of rigid-body states

- pitch acceleration due to elevator "step" (+1 degree)
- roll acceleration due to aileron "stair" (+1°, 0°, -1°, 0°)
- yaw acceleration due to rudder step (+1°)

Figure 2.12-1 compares the different models of flight mechanics with the reference model of aeroelastics A(qs). The differences, mainly in yaw damping, and the influence of elasticity are clearly visible.

Fig. 2.12-2 compares the influence of a different number of elastic modes. It shows the influence of elasticity more clearly. Especially with pitch and roll acceleration, it is visible that with elastic modes the vibrations move around their own average curve but not around the curve of the simple rigid model. This proves again the influence of elasticity on rigid-body movement.

Fig. 2.12-3 compares the results of the integral model I(A(qs)), i.e. (s. § 2.8) rigid-body behavior determined by aeroelastics, $x_{Fr} = x_{Ar}(A(qs))$ with I(F2Lr), i.e. rigid-body behavior determined by flight mechanics, $x_{Fr} = x_F(F2Lr)$.

The differences are rather small. They result from the different rigid-body models.

In addition, one can see clearly that the same elastic vibration is superimposed to the applied rigid-body movement. This proves

again that elasticity can be superimposed by applying equation 2.8-5 if a good rigid-body model is available.

Finally Fig. 2.12-4 shows the measurable acceleration at the pilot seat (model (A(qs))) due to control commands. Here the influence of elasticity is rather large as already shown. The response amplitudes due to rudder step are nearly twice as large as those of rigid a/c, the same applies to the elevator step which introduces a strong response peak right at the beginning.

Naturally, such a large elastic a/c response would be reduced in reality by electronic filtering or by mechanical reduction due to slow actuators. In this simulation no reduction was introduced. The transfer functions of actuators were set to 1=constant with the intention to show the potential of the aircraft.

3. THE INTEGRAL CONTROLLER

3.1 Objectives

There are three different tasks of the integral controller to be distinguished: flight control, load control and mode control. Their objectives are rather different.

In general one can name:

flight control:

- flight stability
- aircraft protection
- maneuverability
- defined flight path following
- reduction of workload of pilot

load control:

- reduction of limit loads
- reduction of fatigue loads
- avoidance of critical failure conditions

mode (or structural vibrations) control

- aeroelastic stability
- minimization of structural vibrations
- improvement of passenger comfort

All these objectives interfere with each other, some are even contradictory to each other, and most of them can be subdivided into a larger number of subobjectives.

Nevertheless, they can be detailed and – with some exceptions – given as criteria in a mathematical formulation. So an integral controller can be designed in a multicriteria optimization process, with targets and constraints.

For the purpose of mode control, which is of main interest in this context, one can distinguish three different types of controller objectives: flutter suppression, flutter margin augmentation and reduction of vibration level for comfort. Flutter suppression would cure a flutter case within the flight envelope. Flutter margin augmentation would cure a flutter case in an area for which the aircraft is not designed but which must be covered as required by law. Comfort control would reduce the natural structural vibrations caused by air turbulence down to a comfortable level on a naturally stable aircraft.

All mode controllers aim at an increase of the damping of structure modes. Their main difference is the required level of safety.

3.2 Requirements and Restrictions for Mode Control

3.2-1 Airworthiness Requirements

For mode controllers the main safety requirements are also airworthiness requirements. For civil aircraft and structural aspects, these are the FAR or JAR 25 requirements, here § 25.629 "Flutter, Deformation and Fail Safe Criteria" and § 25.302 "Interaction at Systems and Structure". If one looks at the flutter speed to be reached a literal interpretation of the requirements leads to Fig. 3.2-1 for its definition. The required speed depends on the system's probability of being in failure. So one can read in Fig. 3.2-1 that:

- ☐ flutter suppression controllers need a probability of being in failure state of $<10^{-9}$, since they have to shift the flutter speed from below VD up to 1.15 VD
- ☐ flutter margin augmentation controllers need $<10^{-5}$, since they have to shift from above VD up to 1.15 VD
- ☐ comfort controllers need <1 , since here the natural a/c reaches already 1.15 VD. If the system fails, there is no safety problem but only a comfort problem which is not the subject of these paragraphs.

A special situation arises if a high speed protection (HSP) system and a mode control (MC) system are used in combination to keep $V \leq V_C$ and to avoid flutter within $V_C < V_F < V_D$. If both systems have an independent probability of being in failure state of $<10^{-5}$,

in combination they can reach a value of $<10^{-9}$, as required. But nevertheless, $V_F < V_D$ if the MC system fails, although VF cannot be reached due to the HSP system.

3.2-2 Mode Control Design Criteria

Any controller should be safe, efficient, robust and should not disturb other positive features of the controlled system.

For safety reasons, the a.m. JAR requirements defined by the flutter speed to be reached must be fulfilled. But there are other safety criteria too.

First the amount of modal damping which indicates a certain stability robustness against scatter, ageing or disturbances.

Second the phase and gain margins (well known for single input/single output (SISO) – systems) which show the robustness against deviations from nominal conditions or against minor failures not especially mentioned.

The efficiency or performance of the controller can very simply be defined in most cases by the flutter velocity or the modal damping to be reached.

The robustness is a more complex issue. One aspect, the "safety robustness" was already mentioned before. Another aspect is "performance robustness" against disturbances or against operation conditions. The number of the latter one is huge. It includes, among others, a/c velocity, altitude, flap/slat setting, payload, fuel and their distributions. Each combination of these conditions defines a load case to be included in the controller design.

Finally it must be shown by the evaluation of time response due to step input or frequency response due to random excitation that the controller neither introduces unwanted features nor reduces wanted features, such as good a/c maneuverability.

In the following some requirements are detailed as a first proposal for a multi-input / multi-output (MIMO) controller.

☐ Flutter control:

For modal damping " ξ_n " of each of n eigenvalues shall be $\xi_n \geq 0.5\%$ (% of critical) and

$$\frac{d\xi_n}{dv} > -0.01 \text{ [% / kts CAS]}$$

This guarantees stability.

☐ Comfort control:

The maximal singular value " $\bar{\sigma}$ " of a number m of pick-up signals " y_m " due to gusts " w " in frequency range " f_1 " to " f_2 " shall be minimal and at least smaller than a limit value $G_{Hym,w}$ i.e.

$$\max(\bar{\sigma}(H_{ym,w}(i\omega))) \rightarrow \min_{f_1 \div f_2}$$

$$\max(\bar{\sigma}(H_{ym,w}(i\omega))) < G_{Hym,w} \quad 0 \div \infty$$

where $H_{ym,w}(i\omega)$ is the transfer function from gust w to the pick-up signal y_m .

This should reduce the response to turbulence.

☐ Robustness of control (based on ref. 7):

The phase margin of the open loop transfer function $H_{u,u}(i\omega)$ of all actuator signals u shall be

$$\frac{30^\circ \cdot \pi}{180} \leq |2 \cdot \arcsin(\min(\underline{\sigma}(1 + H_{u,u}(i\omega))) / 2)|$$

the gain margin of the open loop transfer function $H_{u,u}(s)$ of all actuator signals u shall be

$$1 / (1 - \min(\underline{\sigma}(1 + H_{u,u}(i\omega)))) > 2$$

and

$$1 / (1 + \min(\underline{\sigma}(1 + H_{u,u}(i\omega)))) \leq 0.66$$

where $\underline{\sigma}$ is the minimum singular value.

This should ensure safety robustness.

If these criteria were really met in the whole envelope of velocity and altitude as well as in all loading conditions of fuel and payload, a good controller should be reached.

But these requirements are probably too stringent and some monitored exceptions are therefore necessary. At the moment, there is insufficient experience available to present more details on this issue. But one thing is beyond question: some requirements of this type are necessary.

The mere definition of the required flutter speed, as given in FAR 25.302, is not sufficient. At least a certain amount of robustness is necessary for safety to cover smaller scatter or deviations from

nominal conditions which are not defined as separate failure states.

3.2-3 Reliability / Failure Probability

A good reliability or low failure probability can be reached by different methods. For example, redundancy of hardware installations and signal monitoring are well known. For MIMO controllers studied here, special attention should also be paid to the minimization of interactions between the different signal lanes of the controller.

3.2-4 Safety Restrictions for Mode Control

This could include:

- ☐ Low pass filter for the flight control signal part and band pass filter for the signal part of mode control. This prevents a failure in the more complicated flight controller part from causing flutter problems and a failure in the mode controller part from influencing the flight path.
 - ☐ Decoupling network with diagonal structure of the controller transfer matrix of MIMO systems. This could e.g. be done by superposition of different effective SISO systems which do not interfere with each other.
- If all SISO systems are stable and effective for themselves, a failure and a switch-off of one of these lanes will not lead to a complete loss of the controller.

Admittedly, such measures cannot always be taken. Especially a separation by filter does not work if rigid-body frequencies and elastic mode frequencies are close together. But if it works, these filters should be used under all circumstances. Missing filters present an unnecessary risk.

3.3 Design

The design of the integral controller is a multidisciplinary process of multicriteria optimization. Fig. 3.3-1 may give a survey of its principle structure.

First an integral model of the a/c must be established and made available in linear and nonlinear form for all loading and flight conditions to be covered.

Second a complete list of criteria is to be established, including all objectives of the different disciplines.

Then the question arises how the controller should be structured. In most cases experience answers this question, otherwise, theoretical methods of robust optimal control law design as e.g. the H_∞ method are available to find a good structure.

If the structure is known its parameters can be optimized by a multiobjective optimization strategy.

Finally the resulting controller must undergo a special assessment by the different disciplines, including simulations with pilot in the loop.

Of course, one has to keep in mind that by increasing the number of aims the efficiency of the controller will be reduced.

It is still impossible to get everything simultaneously!

Modifications of controller structure, of criteria or even of control surfaces or systems may be necessary.

The first three iteration steps of an example of such a multicriteria optimization is shown in Fig. 3.3-2 (s. ref. 8) where a limited number of criteria was studied. One can see that finally all criteria are met. The program stops when "pareto optimal" results are reached, i.e. when a value of one criteria can only be improved by impairing another one.

4. CONCLUSION

- ☐ Increasing a/c flexibility requires integral controllers for flight, load and mode control.
- ☐ The controller design must be based on an integral a/c model which covers the requirements of flight mechanics, loads and aeroelastics.
- ☐ The integral model can be based on a classical aeroelastics model if several improvements are introduced.
- ☐ Linear or nonlinear rigid-body motion of traditional flight mechanics can be coupled with structural vibrations of traditional aeroelastics without restrictions.
- ☐ APC can be included.
- ☐ Controller design should be performed by a multiobjective parameter optimization to reach an optimum for all criteria.
- ☐ Safety and design criteria for mode control need further discussion.

Acknowledgement:

This work was partially sponsored by the german BMBF.

REFERENCES

1. K. König "On the New Quality of the Flutter Problem Due to Coupling of Structure and Electronic Flight Controls in Modern Large and Flexible Civil Aircraft" International Forum on Aeroelasticity and Structural Dynamics, Straßbourg, May 24 - 26, 1993
2. J. Schuler "Flugregelung und aktive Schwingungsdämpfung für flexible Großraumflugzeuge" VDI Fortschrittsbericht Reihe 8 Nr. 688 Düsseldorf: VDI Verlag 1998
3. R. Vepa "On the Use of Padé Approximants to Represent Unsteady Aerodynamic Loads for Arbitrarily Small Motions of Wings", Proceedings of the AIAA 14th Aerospace Sciences Meeting, AIAA Paper No. 76-17, Washington, D.C., January 26-28, 1976.
4. K.L. Roger "Airplane Math Modeling Methods for Active Control Design, AGARD-CP-228, pp. 4.1-4.11., August, 1977
5. M. Karpel and E. Strul "Minimum - State Unsteady Aerodynamic Approximations with Flexible Constraints, Proceedings of the International Forum on Aeroelasticity and Structural Dynamics, pp. 66.1-66.8, Manchester, June 26 - 28, 1995
6. L. Böger et. allied "Experimentelle Ermittlung der kinematischen Rückkopplung des Piloten aufgrund von Cockpit Beschleunigungen", DGLR - JT 98-008 p.753-762, Bremen, October 6th, 1998
7. N.A. Lektomaki, N.R. Sandell Jr., M. Athans "Robustness Results in Linear-Quadratic Gaussian Based Multivariable Control Design", IEEE Transactions on Automatic Control, vol. AC-26 No. 1, p. 75-93, February, 1981
8. G. Grübel et. allied "ANDECS / MOPS 3.0 Tutorials" DLR Oberpfaffenhofen, July 1995

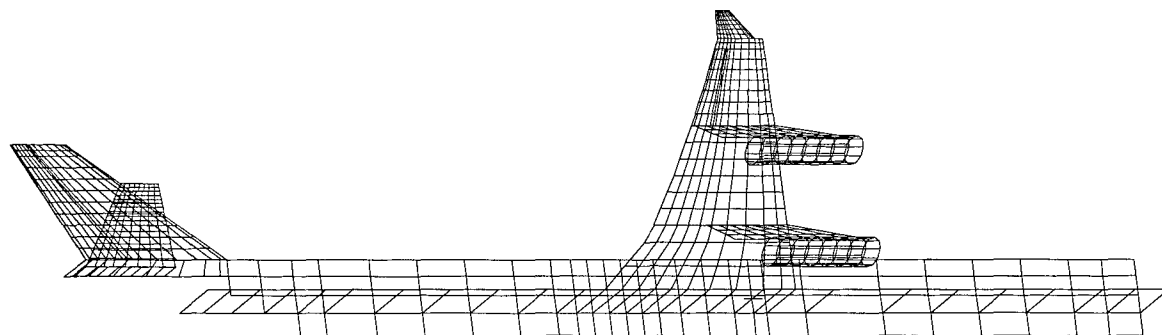


FIG. 2.1-1: MODELING OF FUSELAGE FOR AIR LOADS

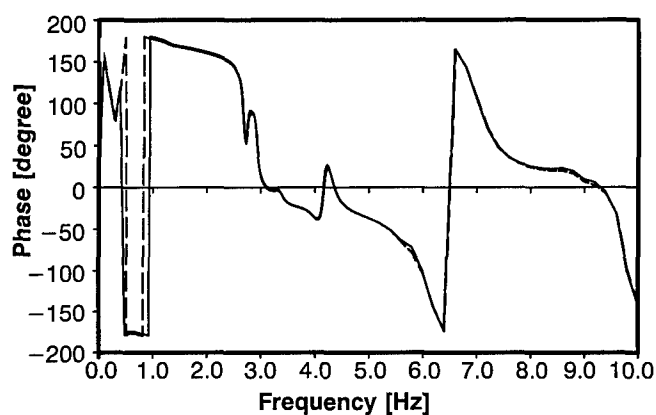
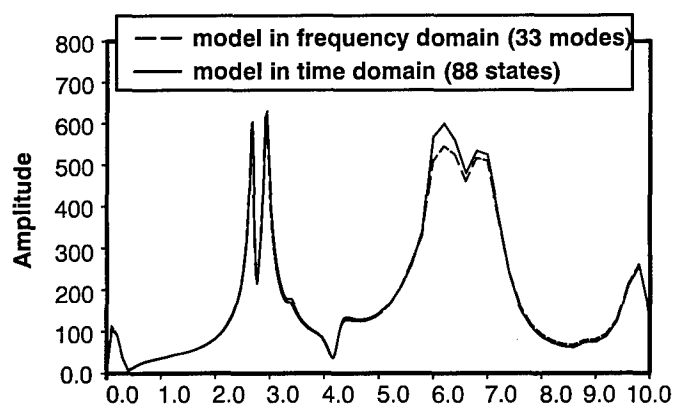


FIG. 2.7-1 TRANSFER FUNCTION FROM ELEVATOR TO FRONT FUSELAGE ACCELERATION

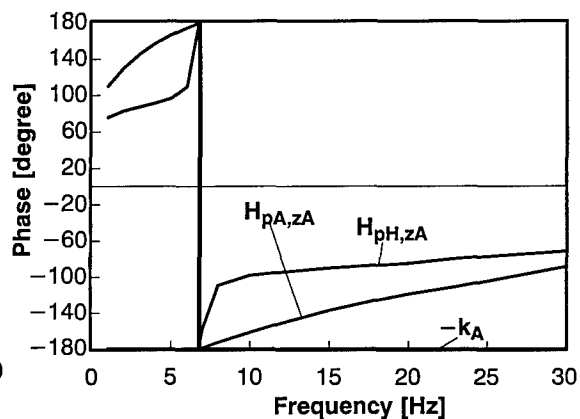
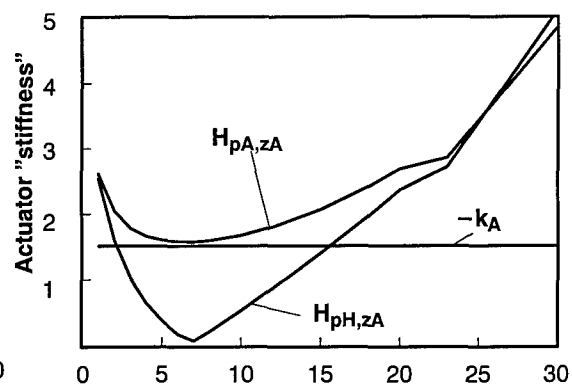


FIG. 2.9-1: ACTUATOR TRANSFER FUNCTIONS OF DISTURBANCE OR FLEXIBILITY

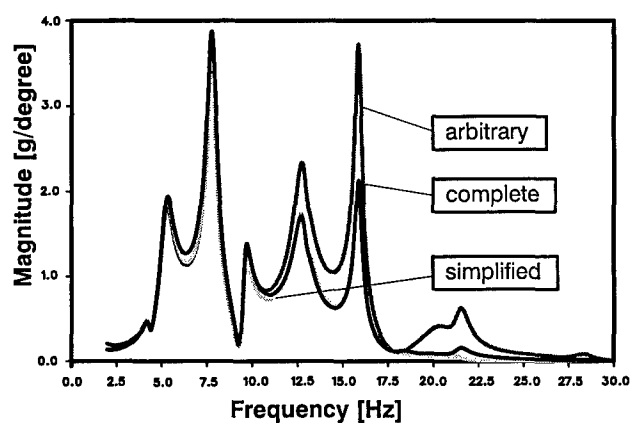


FIG. 2.9-2
H_{Z,u} TRANSFER FUNCTION FROM ELEVATOR TO WING TIP
INFLUENCE OF ACTUATOR MODEL

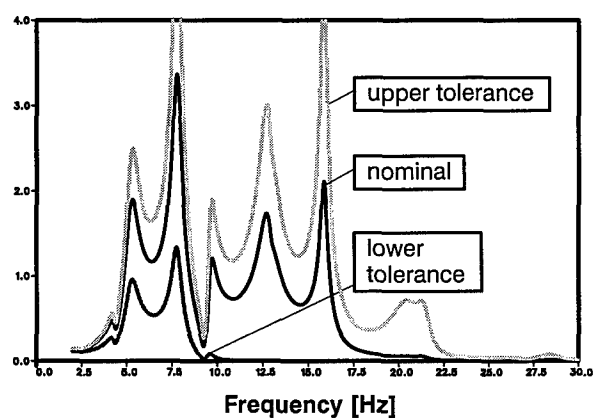


FIG. 2.9-3
H_{Z,u} TRANSFER FUNCTION FROM ELEVATOR TO WING TIP
INFLUENCE OF ACTUATOR SCATTER

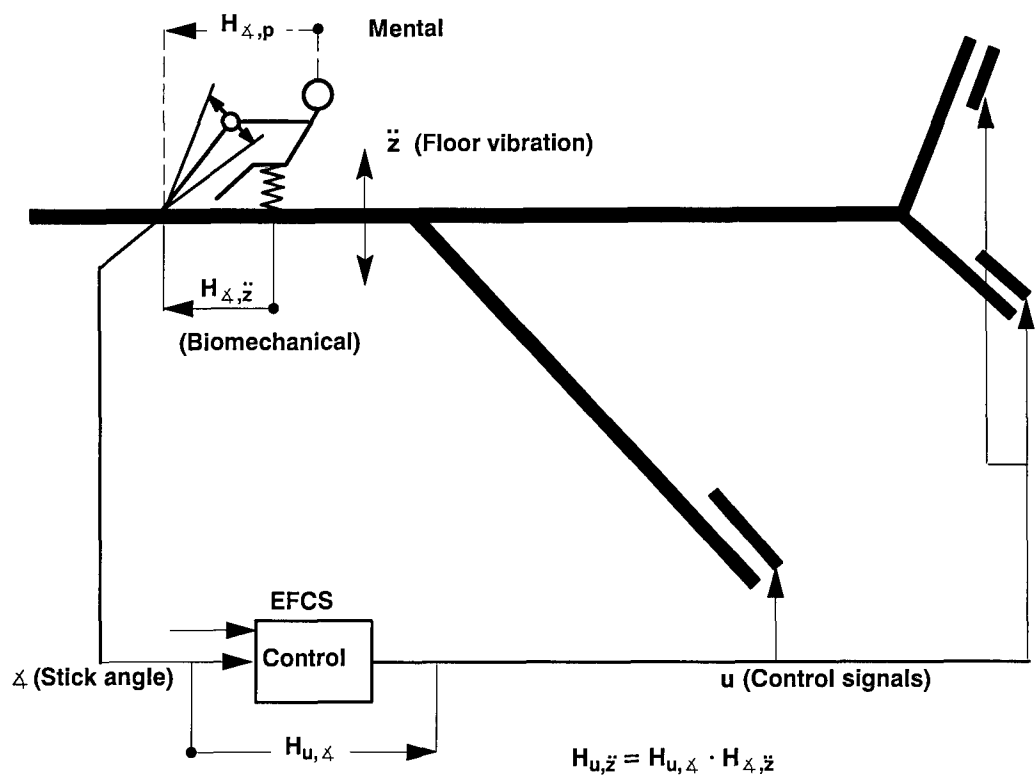


FIG. 2.11-1: AIRCRAFT PILOT COUPLING MECHANISM

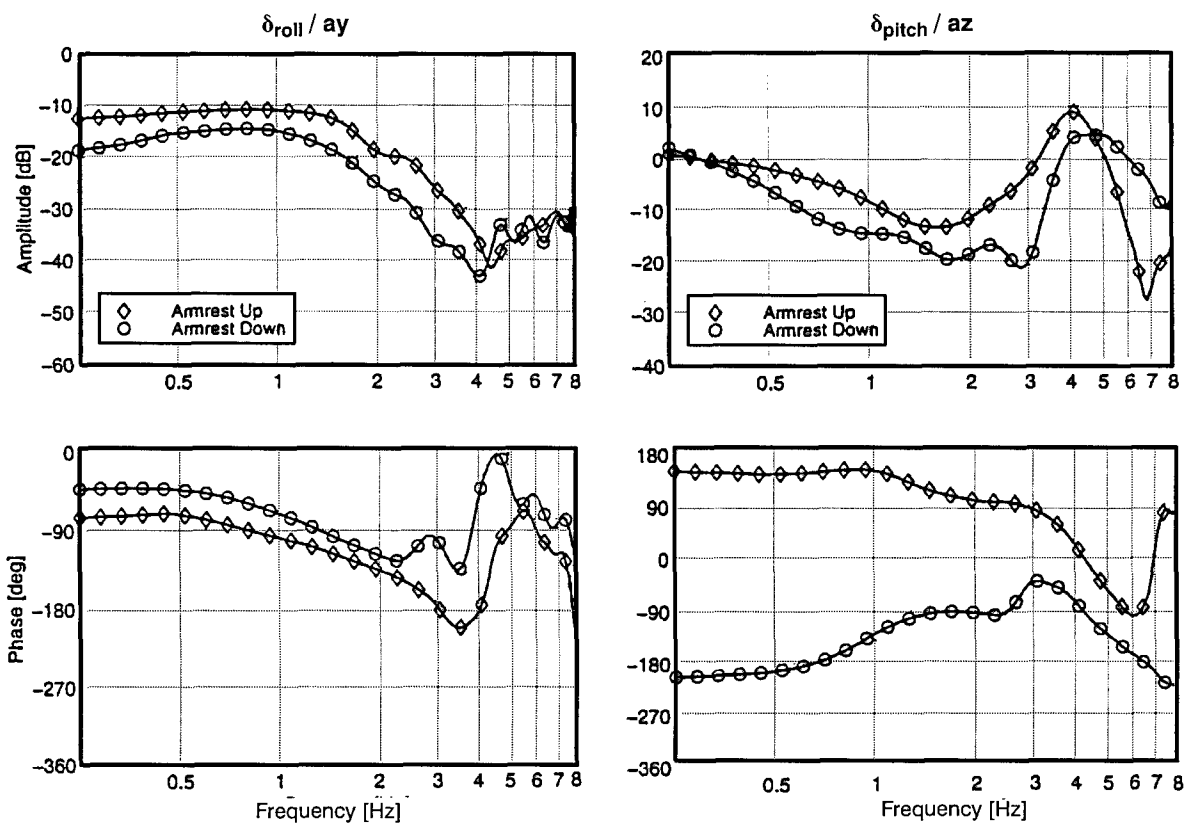


FIG. 2.11-2: TRANSFER FUNCTION FROM A/C FLOOR VIBRATION TO SIDE STICK MOVEMENT

		phygoid	dutch roll	short period
A(qr)	fn [Hz]	0.01076	0.1596	0.2442
	ξn [%]	5.22	10.70	48.76
A(qs)	fn [Hz]	0.01160	0.1551	0.2202
	ξn [%]	7.30	10.87	48.96
A(qc)	fn [Hz]	0.01232	0.1480	0.1876
	ξn [%]	8.14	10.01	51.87
F1Lr	fn [Hz]	0.007706	0.1640	0.1694
	ξn [%]	-8.05	11.20	55.08
F2Lr	fn [Hz]	0.009915	0.1685	0.2105
	ξn [%]	2.65	6.83	52.72
F2Le	fn [Hz]	0.01140	0.1630	0.1391
	ξn [%]	2.01	2.17	68.26

TABLE 2.12-1: EIGENVALUES OF INTEGRAL MODELS

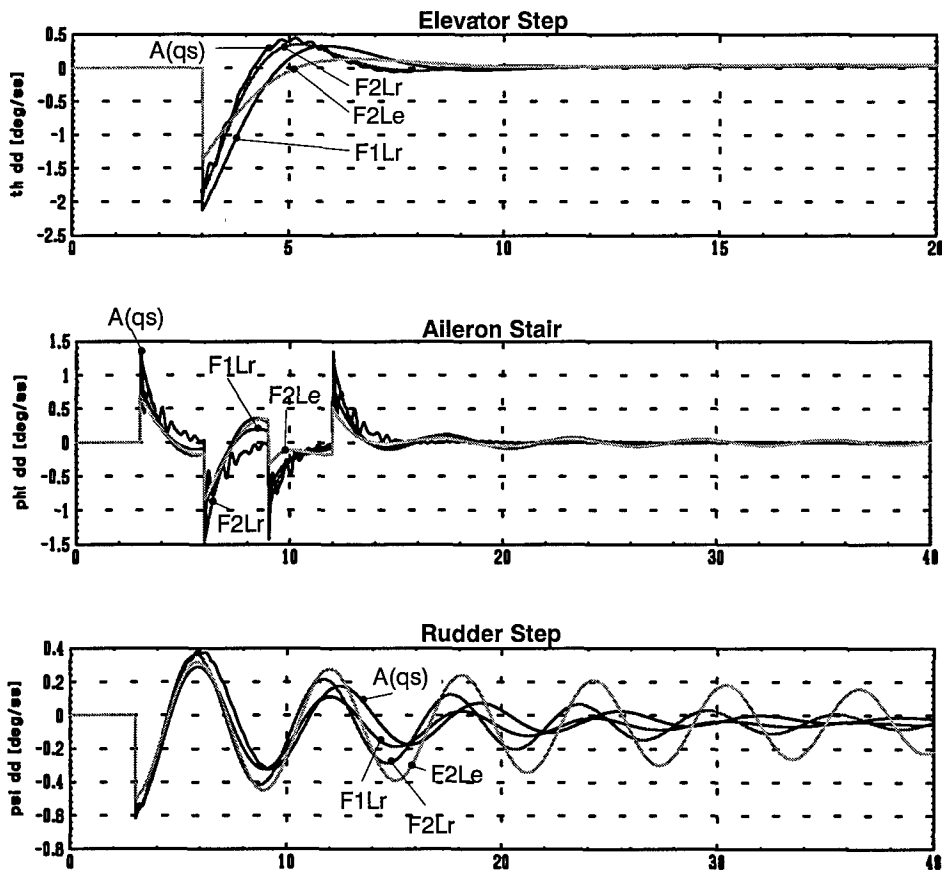


FIG. 2.12-1: ACCELERATION RESPONSE TO CONTROL COMMAND (Comparison of Data)

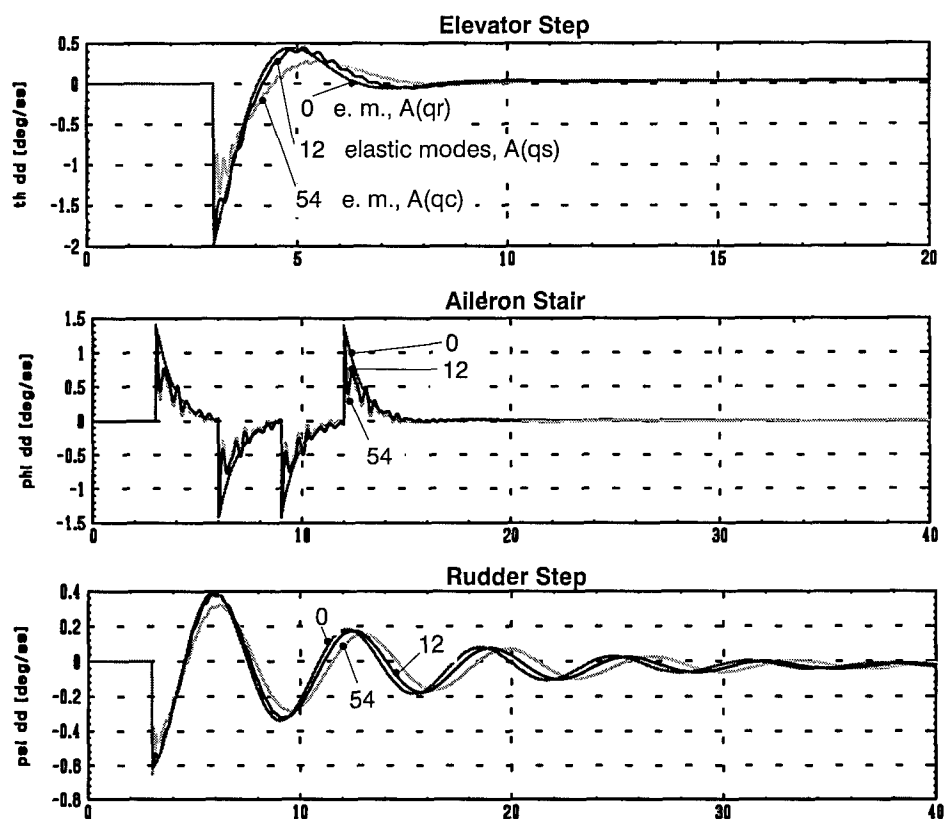


FIG. 2.12-2: ACCELERATION RESPONSE TO CONTROL COMMAND
(Influence of Number of Elastic Modes
on Rigid-Body State Response)

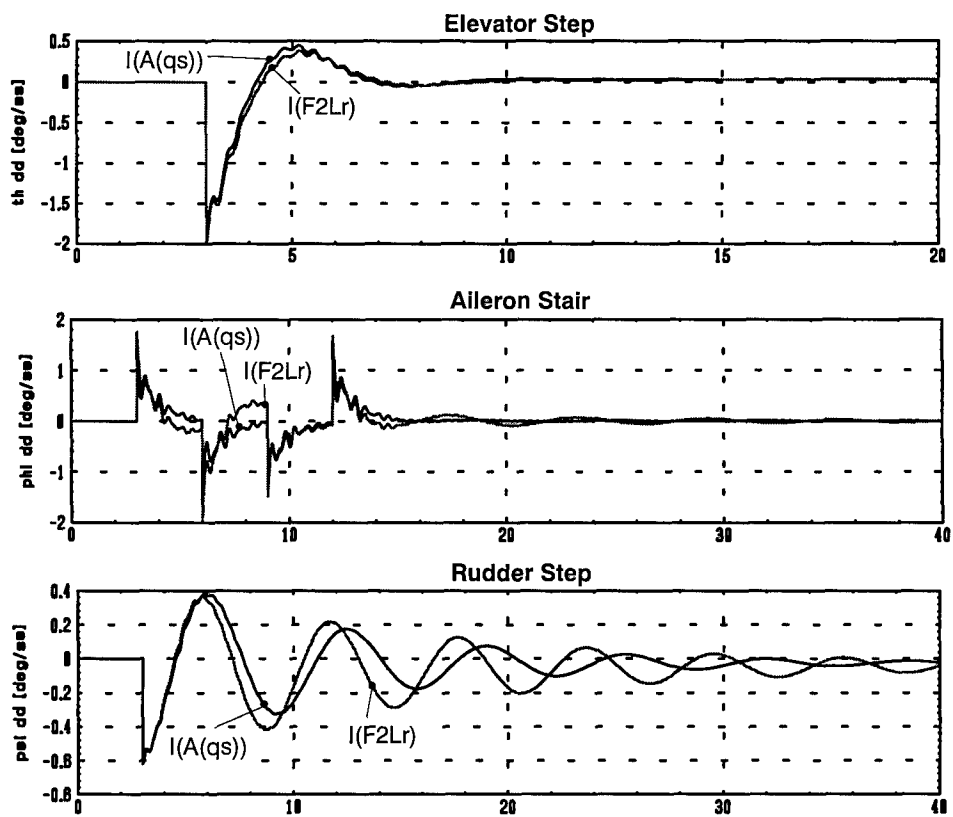


FIG. 2.12-3: ACCELERATION RESPONSE TO CONTROL COMMAND
(Comparison of Integral Models Based on Aeroelastics $A(qs)$
and on Flight Mechanics $F2Lr$)

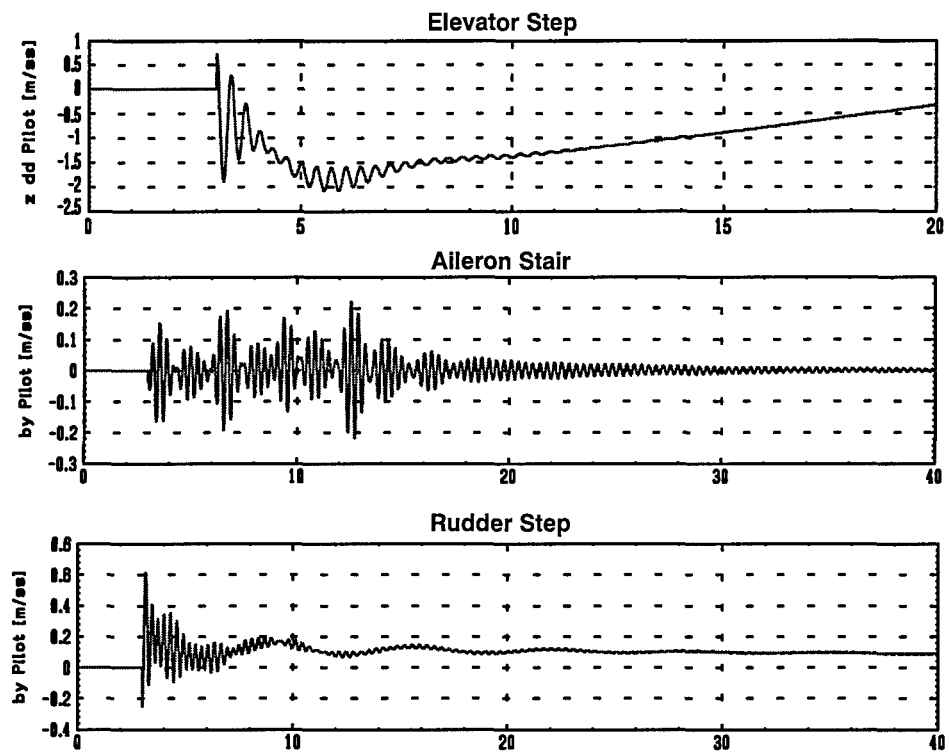
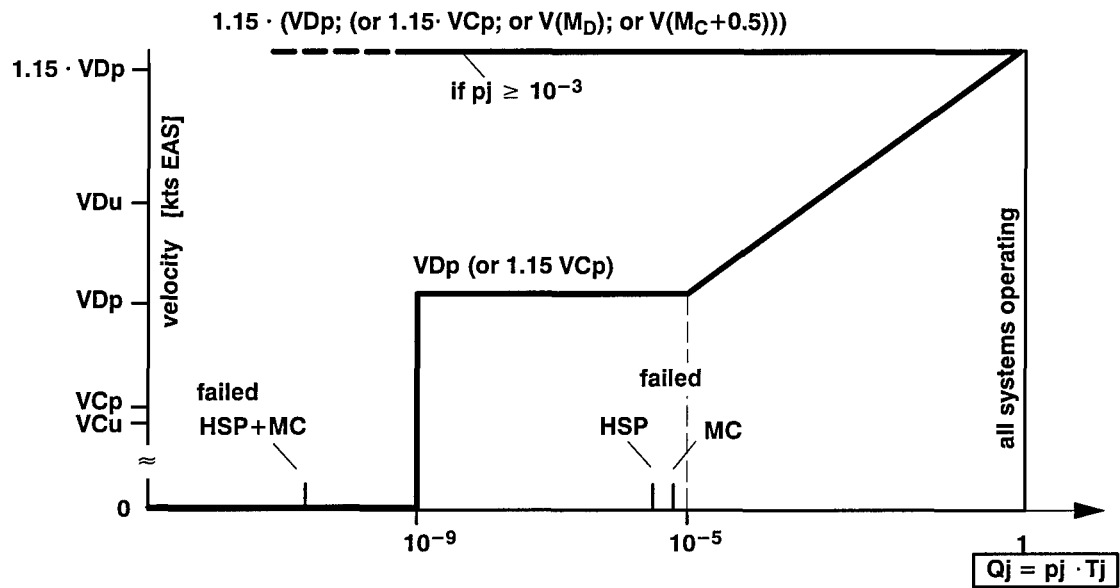


FIG. 2.12-4: PILOT ACCELERATION IN ELASTIC A/C



Probability of being in failure state $Q_j = p_j \cdot T_j$ with average time T_j spent in failure condition and p_j probability of occurrence of failure mode per flight hour.

e.g.:
 $VD_u - VC_u \approx 60$ kCAS unprotected
 $VD_p - VC_p \approx 35$ kCAS protected

FIG: 3.2-1: REQUIRED FLUTTER SPEED (NPA 25C-199/ACI 25.302 § 4.1.2.2)

